

Identification of undocumented buildings in cadastral data using remote sensing: Construction period, morphology, and landscape

Qingyu Li^{a,b}, Hannes Taubenböck^{c,d}, Yilei Shi^e, Stefan Auer^b, Robert Roschlau^f, Clemens Glock^f, Anna Kruspe^a, Xiao Xiang Zhu^{a,b,*}

^a Data Science in Earth Observation, Technical University of Munich (TUM), Arcisstr. 21, 80333 Munich, Germany

^b Remote Sensing Technology Institute (IMF), German Aerospace Center (DLR), Oberpfaffenhofen, 82234 Wessling, Germany

^c Remote Sensing Data Center (DFD), German Aerospace Center (DLR), Oberpfaffenhofen, 82234 Wessling, Germany

^d Institute for Geography and Geology, University of Würzburg, 97074 Würzburg, Germany

^e Remote Sensing Technology (LMF), Technical University of Munich (TUM), Arcisstr. 21, 80333 Munich, Germany

^f Bavarian Agency for Digitization, High-Speed Internet and Surveying (LDBV), Alexanderstr. 4, 80538 Munich, Germany

ARTICLE INFO

Keywords:

Undocumented building
Building morphology
Building landscape
Remote sensing
Deep learning

ABSTRACT

Buildings are the predominant objects that characterize the urban structure. For many cities, local governments establish building databases for administration as well as urban planning and monitoring. However, newly constructed buildings are often only included with a considerable time delay in the official digital cadastral maps due to processes in the acquisition of data, so-called undocumented buildings. In this regard, detecting undocumented buildings using remote sensing techniques would support the construction of up-to-date building databases with complementary information. In-depth studies on undocumented buildings and their number and location, however, are scarce. Therefore, we exploit a deep learning-based framework to detect undocumented buildings in remote sensing data and propose to derive 2D and 3D morphological parameters as well as landscape metrics., which are capable of depicting the physical forms and spatial structures of undocumented buildings. Furthermore, we exemplify the variabilities of undocumented buildings across space by the differences in morphology and landscape metrics between high and low building density regions. Upon analysis of undocumented buildings in 15 cities in the state of Bavaria, Germany, both state- and city-scale results reveal that most undocumented buildings are located in lower dense regions. This reveals that fragmentation of the landscape by building structures in the state of Bavaria is probably greater than official geospatial data currently documented.

1. Introduction

The three-dimensional (3D) building stock characterizes the planar and vertical dimensions of built structures where people live (Cao and Huang, 2021). The construction of 3D building models in nowadays administrations of communities allows for administrating, documenting, and monitoring urban development (Li et al., 2020b). Across the globe, some cities already have building databases for resource management (Griffiths and Boehm, 2019). For instance, in most German cities, a two-dimensional (2D) building database, namely, digital cadastral map (DFK), is provided by the official authority. The geographic coordinates of buildings documented in the DFK are acquired through terrestrial surveys, which provide accurate and comprehensive information for sustainable urban planning. As more and more houses are

being built, the conversion from natural land into urban land is an ever-going process (Taubenböck et al., 2012; Huang et al., 2021; Huang et al., 2022). In most cases, there are buildings newly constructed in former arable land, pastures, forests, etc (Leichtle et al., 2017). Therefore, monitoring newly constructed buildings is helpful to support sustainable land resource management (Huang et al., 2020). Nevertheless, some newly constructed buildings are not recorded in an up-to-date manner via terrestrial surveying. Since these buildings are missing in the DFK, they are named “undocumented buildings”.

Remote sensing technologies such as airborne imaging and laser scanning make it possible to identify these undocumented buildings, as they provide high-resolution data sets for detailed analysis of buildings on a large scale. Early efforts (Roschlau et al., 2020; Geßler

* Corresponding author at: Data Science in Earth Observation, Technical University of Munich (TUM), Arcisstr. 21, 80333 Munich, Germany.

E-mail addresses: qingyu.li@tum.de (Q. Li), hannes.taubenboeck@dlr.de (H. Taubenböck), yilei.shi@tum.de (Y. Shi), stefan.auer@dlr.de (S. Auer), Robert.Roschlau@ldbv.bayern.de (R. Roschlau), Clemens.Glock@ldbv.bayern.de (C. Glock), anna.kruspe@tum.de (A. Kruspe), xiaoxiang.zhu@dlr.de (X.X. Zhu).

et al., 2019) have been developed for the detection of undocumented buildings, which first extract buildings based on heuristic methods and then overlay the extracted building maps on the DFK to detect undocumented buildings. However, the heuristic thresholds utilized in these strategies cannot guarantee a uniform and standardized processing manner, limiting their application on a large scale. Moreover, results obtained from these approaches show a high false alarm rate (Li et al., 2020a). Recently, a novel framework (Li et al., 2020a) has been proposed to detect undocumented building constructions. In this method, buildings are first extracted by convolutional neural networks (CNNs), as CNNs have better generalization capability than heuristic methods (Li et al., 2020a; Zhu et al., 2017). After the comparison with the DFK, it has been shown that undocumented buildings can be detected with high accuracy. Furthermore, this framework is able to acquire the construction period of undocumented buildings in multi-temporal remote sensing data, which provides complementary information for urban planning.

Morphology parameters of buildings provide a quantitative characterization of urban morphology and facilitate the analysis of the sustainability, efficiency, and resilience of a city (Bonczak and Kontokosta, 2019). Morphology analyses are carried out in two ways, (1) 2D (e.g., building area) and (2) 3D (e.g., building volume) (Yoshida and Omae, 2005). The derived 2D and 3D building morphological parameters contribute to the analysis in different aspects, e.g., urban structures (Taubenböck et al., 2017), energy consumption (Kontokosta and Tull, 2017), solar radiation acquisition (Robinson, 2006), pedestrian wind flow modeling (Kubota et al., 2008), or surface thermal efficiency and loss (Lu et al., 2019). Landscape metrics capturing spatial parameters of buildings are exploited for quantitative observation of landscape patterns, which offer a way to explore the landscape's ecological processes. 2D building landscape metrics (e.g., mean building area) are widely examined in many studies, however, they are still biased when dealing with complex scenes and high height heterogeneity (Cao et al., 2020). 3D building landscape metrics (e.g., floor area ratio) take the vertical features into consideration, providing a more comprehensive understanding of landscape patterns (Taubenböck et al., 2016). The landscape analysis of buildings reveals the urban landscape pattern characteristics that have impacts on ecosystems (Wu, 2014), air quality (Lu and Liu, 2016), public health (Koohsari et al., 2015), etc. Therefore, morphological parameters and landscape metrics of the undocumented buildings are of crucial interest to administration, urban planning, and science, as in-depth studies can provide insights into land use, and sustainable development, among others.

During the process of construction of buildings especially in and around urban areas, one of the most urgent problems is urban sprawl. Urban sprawl is usually linked to the low density growth of urban space (Hamidi and Ewing, 2014; Durieux et al., 2008). This relates to negative impacts on urban sustainability, including excessive car use, high costs of infrastructure, and lack of social interaction (Abdullahi et al., 2018). However, if building databases are incomplete, the analysis regarding urban sprawl will also be biased. In this paper, we propose to quantify undocumented buildings with respect to high and low building density regions. With it, we inspect their effects on morphological characteristics and landscape patterns. Specifically, we want to show whether the number of undocumented buildings is higher in high-density or low-density regions and thus show what influence this has on the assessment regarding urban sprawl.

In this study, we propose to investigate these effects by monitoring construction period, morphology, and landscape of undocumented buildings. The contributions of this article are twofold:

(1) We propose to utilize a set of 2D and 3D metrics to carry out morphology and landscape analysis of undocumented buildings, which can provide insights for environmentally sustainable development.

(2) We propose to investigate the differences in morphology parameters and landscape metrics of undocumented buildings between high and low building density regions. The results can provide empirical evidence relating to the extent of urban sprawl, and are helpful for policy-makers to control this problem.

Table 1

Datasets utilized for this research. In this research, time point 1 is the year 2014, while time point 2 is the year 2017.

Dataset	Temporal information
nDSM	Time point 2
tDSM	Within the period from time point 1 to time point 2
TrueDOP	Time point 2
DFK	Time point 2

2. Data and methodology

2.1. Study regions

The study regions are located in the state of Bavaria, Southeast Germany. Due to the availability and accessibility of datasets, 15 cities are selected and distributed across the federal state (see Fig. 1). The selected 15 cities are Wolfratshausen, Weilheim, Schweinfurt, Wasserburg, Rosenheim, Regensburg, Muenchen, Landshut, Landau, Kronach, Kulmbach, Hemau, Deggendorf, Bad Toelz, and Ansbach, which host about 3 million inhabitants. Muenchen is the largest city. The spatial extents of cities are defined by the administrative boundaries. The selected 15 cities vary in geographical, social, and economic conditions. Hence, the investigation of these cities can basically be assumed to be representative of the various patterns existent.

2.2. Data sets

This study is based on four data sources: (1) a normalized digital surface model (nDSM), (2) a temporal digital surface model (tDSM), (3) orthophotos (TrueDOP), as well as (4) a DFK. For each city, these data are prepared as plenty of tiles with a size of 2500 × 2500 pixels at a spatial resolution of 40 cm/pixel. Fig. 2 illustrates the sample datasets with temporal details shown in Table 1.

(1) **nDSM:** nDSM is the difference model between the digital surface model (DSM) and the digital terrain model (DTM), illustrating objects including trees and buildings. The DSM captures the heights of the Earth's surface including natural and human-made objects and is obtained by a dense matching method (Ressl et al., 2016) from aerial images that are acquired in the year 2017. The DTM is derived as regular point grids from airborne laser scanning (ALS). The accuracy of the DSM and the DTM is ±1.50 m and ±0.2 m, respectively.

(2) **tDSM:** tDSM is the difference between two nDSMs collected at two temporal, i.e., time point 1 (the year 2014) and time point 2 (the year 2017).

(3) **TrueDOP:** TrueDOP are orthophotos with red, green, and blue bands and are collected in the year 2017. All elevated objects including buildings in the TrueDOP have no geometric distortion. This is because that ortho-projection and geo-localization are established on the DSM.

(4) **DFK:** DFK is the building footprint map where the cadastral 2D ground plans of individual buildings are documented via terrestrial surveying in the field. Note that it has high accuracy in the range of centimeters.

2.3. Methodology

2.3.1. The framework of undocumented building detection

In the conceptualization of our study, undocumented buildings refer to the buildings that have been detected in the latest remote sensing data (the TrueDOP and the nDSM) but have not been recorded in the DFK. In this research, we implement a technique proposed in (Li et al., 2020a) for the detection of undocumented buildings. Moreover, this framework can identify the construction period of these undocumented buildings by distinguishing between new undocumented buildings and old ones.

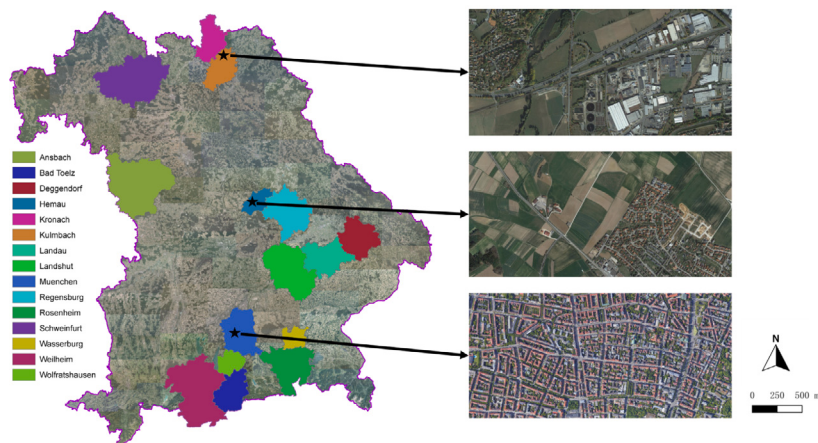


Fig. 1. The study area in this research, which cover 15 cities in the state of Bavaria, Germany.

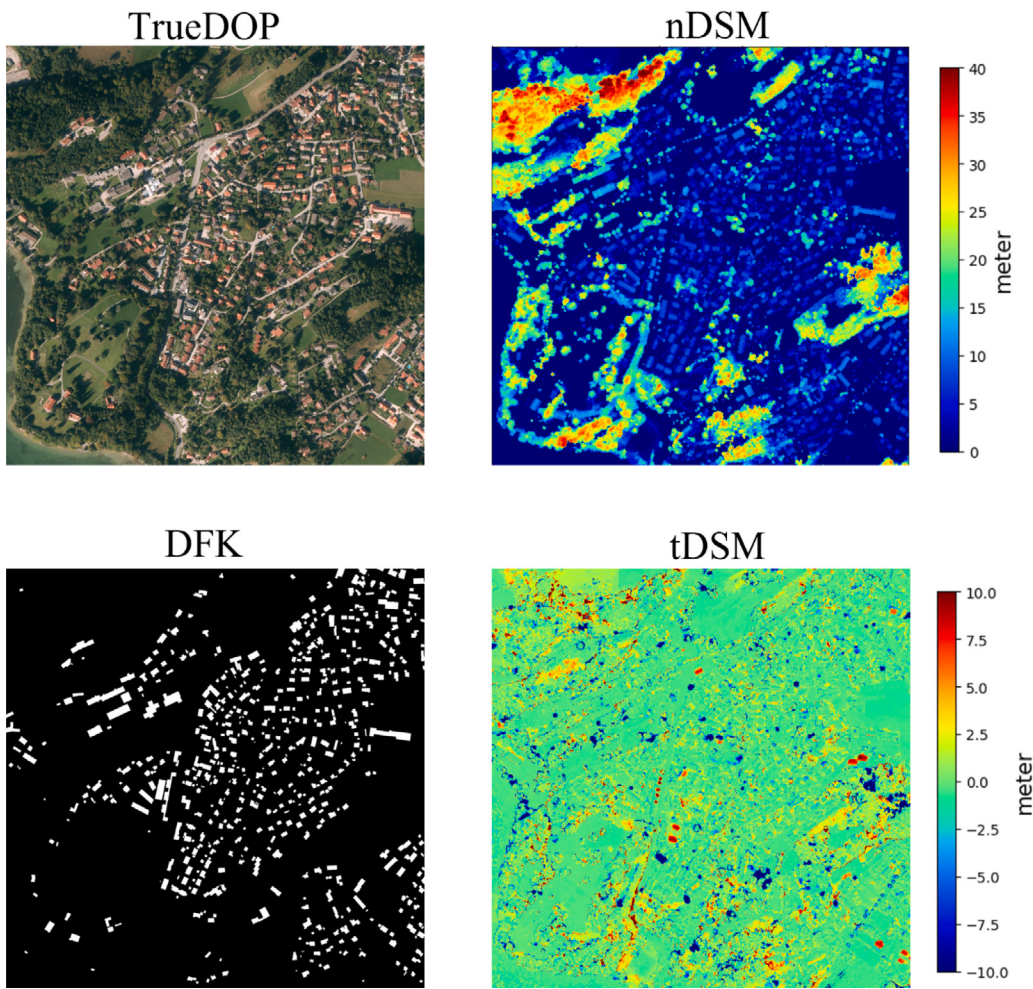


Fig. 2. Sample data from the TrueDOP, the nDSM, the rasterized DFK, and the tDSM.

Fig. 3 presents an overview of this framework, which can be divided into three sub-tasks: (1) building detection, (2) undocumented building detection, and (3) discrimination between new undocumented buildings and old ones.

(1) **building detection:** The latest TrueDOP and the nDSM data are exploited as the two main data sources to detect buildings. The TrueDOP and the nDSM are able to provide spectral and geometrical information about buildings. Therefore, the TrueDOP and the nDSM

data are stacked together as input for the task of building detection, which takes full advantage of both data sources. Recently, CNNs have shown superior performance for the task of building detection when compared to traditional methods. This is because they can automatically learn discriminative features from massive quantities of data, avoiding manual feature selection. FC-DenseNet ([Jégo et al., 2017](#)) is selected as the base CNN model, which assigns every pixel with the label of “building” or “non-building”. FC-DenseNet ([Jégo et al., 2017](#))

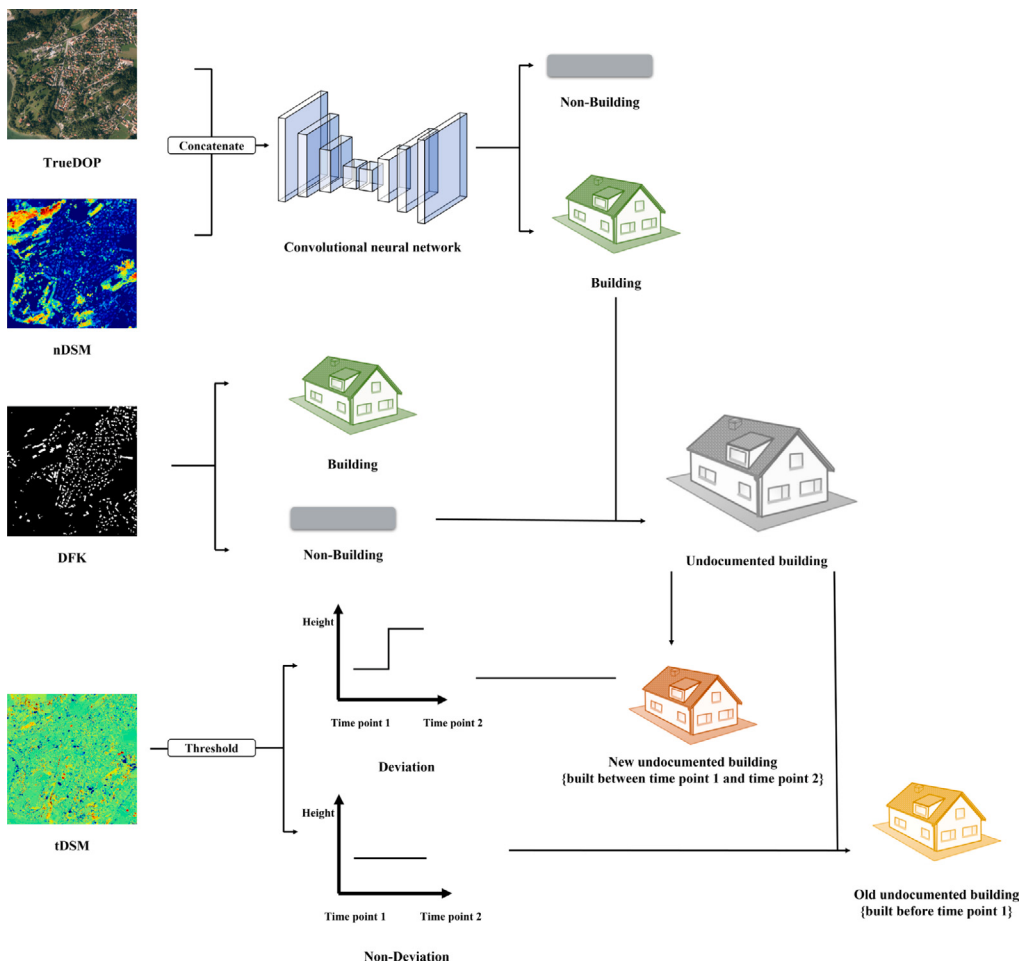


Fig. 3. Overview of the framework of undocumented building detection. Note that a variety of deep learning networks (e.g., FCN-8s (Long et al., 2015), U-Net (Ronneberger et al., 2015), DeepLab V3+ (Chen et al., 2018), HA U-Net (Xu et al., 2021), and FC-DenseNet (Jégou et al., 2017)) can be utilized as the convolutional neural network module in this framework.

is an encoder-decoder architecture, where both the encoder and the decoder are comprised of five dense blocks (Huang et al., 2017). In each dense block, the features are combined by iterative concatenation, providing a more efficient flow for information transmission.

(2) **undocumented building detection:** Once the building footprint maps are generated from the predictions of the FC-DenseNet (Jégou et al., 2017), they are overlaid over the DFK. By doing so, the undocumented building pixels are identified through pixel-wise comparison. Specifically, undocumented building pixels refer to those pixels that are identified as “building” by FC-DenseNet (Jégou et al., 2017). However, in the DFK they belong to the “non-building” thematic class. To mitigate the error accumulation induced from the pixel-wise comparison, we use “Opening”, which is a mathematical morphology operation to alleviate noise (Said et al., 2016).

(3) **discrimination between new undocumented buildings and old ones:** In this study, we classify the detected undocumented buildings into two temporal classes according to their construction period. One type is the old undocumented building that was built before time point 1. The other type is new undocumented building, which refers to the undocumented buildings that were built between time points 1 and 2. In order to identify the construction period, the tDSM is utilized to acquire temporal information. The tDSM shows the difference between two nDSMs that are obtained from time point 1 and time point 2. An empiric threshold (1.8 m) is utilized on the tDSM to check a height deviation within the monitoring period. We apply this threshold as the land surveying team in the Bavarian Agency for Digitization, High-Speed Internet, and Surveying (LDBV), utilizes this value for a standard

garage without a roof usually: it has a minimum height of 1.8 m. Therefore, we select 1.8 m as a threshold to identify whether a building was constructed. Once these undocumented building pixels show height deviation within this period, it is allocated to the thematic class of “new undocumented building”. Otherwise, the identified thematic class should be “old undocumented building”.

The performance of the implemented framework is investigated from two aspects. On the one hand, two popular metrics, intersection over union (IoU) and F1 score (Li et al., 2020a), are utilized for the accuracy assessment of buildings that are extracted by the CNN. On the other hand, the precision is exploited to measure the correctness of detected undocumented buildings in a more targeted manner, which can be computed as follows:

$$\text{precision} = \frac{TP}{P}, \quad (1)$$

where TP refers to the number of correctly detected undocumented buildings and P denotes the number of undocumented buildings that have been detected by the implemented framework.

2.3.2. The definition of high and low building density regions

In this study, we aim to analyze whether there are differences in undocumented buildings across space. Therefore, we conceptualize the space with respect to the pattern of buildings, which is defined as “high” and “low” building density regions. This is due to the fact that we want to show whether the number of undocumented buildings is higher in high density or low density regions and thus show what influence this has on the assessment regarding urban sprawl. Based on

Table 2
Morphological parameters metrics proposed to describe undocumented buildings.

Name	Abbreviation	Equation	Description
Building area	A	$A = \sum_{i=1}^m A_i$	Total area of buildings in one region
Building volume	V	$V = \sum_{i=1}^m V_i$	Total volume of buildings in one region

where m is the number of buildings; A_i and V_i are the area and volume of a building i , respectively.

Table 3
Landscape metrics proposed to describe undocumented buildings.

Name	Abbreviation	Equation	Description
Mean building area	MBA	$MBA = \frac{\sum_{i=1}^m A_i}{m}$	Average of building area in one region
Standard deviation of building area	SDBA	$SDBA = \sqrt{\frac{\sum_{i=1}^m (A_i - MBA)^2}{m}}$	Standard deviation of building area in one region
The number of buildings	NB	$NB = m$	Total number of buildings in one region
The number of high buildings	NHB	$NHB = n$	Total number of buildings over 22.5 m in one region
Mean building height	MBH	$MBH = \frac{\sum_{i=1}^m H_i}{m}$	Average of building height in one region
Standard deviation of building height	SDBH	$SDBH = \sqrt{\frac{\sum_{i=1}^m (H_i - MBH)^2}{m}}$	Standard deviation of building height in one region

where m is the number of buildings in one region; A_i and H_i are the area and the height of a building i , respectively. In our study, H_i is derived as the mean value of the nDSM value of building pixels within i .

the generated building footprint maps from the CNN, we first calculate the building density within each grid cell with a size of 100 m×100 m. By analyzing the building density, we classify these grid cells into 5 types, including very low, low, medium, high, and very high dense regions. In other words, the goal to classify high and low building density regions can be realized by clustering all the grid cells that compose the entire test regions, into 5 categories. To overcome the dichotomous conceptualization of the two abstract classes of “high” and “low”, we conceptualize five thematic density classes of different building density regions, incorporating the transition areas between high and low dense regions. Since the configuration and distribution of transition areas are complex (Zhou et al., 2004), the five thematic classes allow a more differentiated and fine-grained analysis.

To identify the 5 categories, we utilize two methods for the clustering of grid cells within the 15 cities. One method is the commonly used K-means clustering (Hartigan and Wong, 1979), which aims to minimize the difference among the units in each category. K-means clustering exploits the distance as a similarity index, where a shorter distance among two samples represents a larger similarity. By doing so, each cluster is more compact and independent. In our research, the distance is measured by the differences in the building density among grid cells. The other method is equal interval classification (Tyner, 2014), which classifies all grid cells into different categories, and the value ranges in each class are set equal. In other words, the entire range of values (max minus min) is divided equally into the defined number of classes.

2.3.3. Morphological parameters and landscape metrics of buildings

The structure of individual building objects can be characterized by both horizontal and vertical configurations, e.g., area, volume, and height. The spatial aggregation of these configurations of individual buildings in larger geographical extents (e.g., block-level and city-level) allows for capturing spatial patterns of buildings on a larger scale.

Two morphological parameters (cf. Table 2) are used to represent 2D and 3D urban morphology in this paper, respectively: building area and volume. The building area and volume involve the quantitative information in the planar and vertical dimensions, respectively. Building volume offers a more accurate or discriminatory description of urban morphology. This can be illustrated by a town center and a metropolitan area. Both regions might have similar building areas, while the building volumes are substantially different due to the variation of building heights (Chen et al., 2014).

For 2D and 3D landscape analysis, six metrics are selected (cf. Table 3), including the standard deviation of building area, mean building area, the standard deviation of building height, mean building

Table 4
The numbers of training and validation patches for the 14 selected cities.

City	Number of training patches	Number of validation patches
Wolfratshausen	14,982	3671
Weilheim	76,959	19,202
Schweinfurt	54,951	13,759
Wasserburg	14,150	3567
Rosenheim	59,141	14,789
Regensburg	47,947	11,941
Muenchen	88,364	22,213
Landshut	60,957	15,090
Landau	34,964	8733
Kronach	19,987	5112
Kulmbach	24,998	5679
Hemau	9481	2243
Deggendorf	38,454	9763
Ansbach	67,965	18,077

height, the number of high buildings, and the number of buildings. The height value of buildings can be derived from the nDSM, which facilitates the vertical landscape analysis of buildings. Mean building height and mean building area are able to well depict the general structures of buildings in the vertical and horizontal directions, respectively (Chen et al., 2014). The area and height deviation are indicators of heterogeneity of buildings, offering a better understanding of general building structures in the study site (Liu et al., 2017). The number of buildings represents the quantity of building objects in one region, and it can reveal the structural differences among various regions (Chen et al., 2014). We use the metric, the number of high buildings because they are a distinctive feature of the city structure. In our research, a high building is a building with a height larger than 22.5 m (Cao et al., 2020).

3. Results and interpretation

3.1. Quantitative and qualitative results of undocumented buildings

In the implemented framework, the CNN is a crucial module that affects the final undocumented building detection results. All the official geodata are preprocessed to collect small patches for training the CNN. Specifically, all the tiles of the TrueDOP and the DFK as corresponding ground references are clipped into patches with a size of 256 × 256 pixels. Afterwards, we collect the patches from 14 cities in the state of Bavaria, Germany, and we split the collected patches into training and validation subsets for each city. Table 4 shows the number of training and validation patches for the 14 selected cities. To

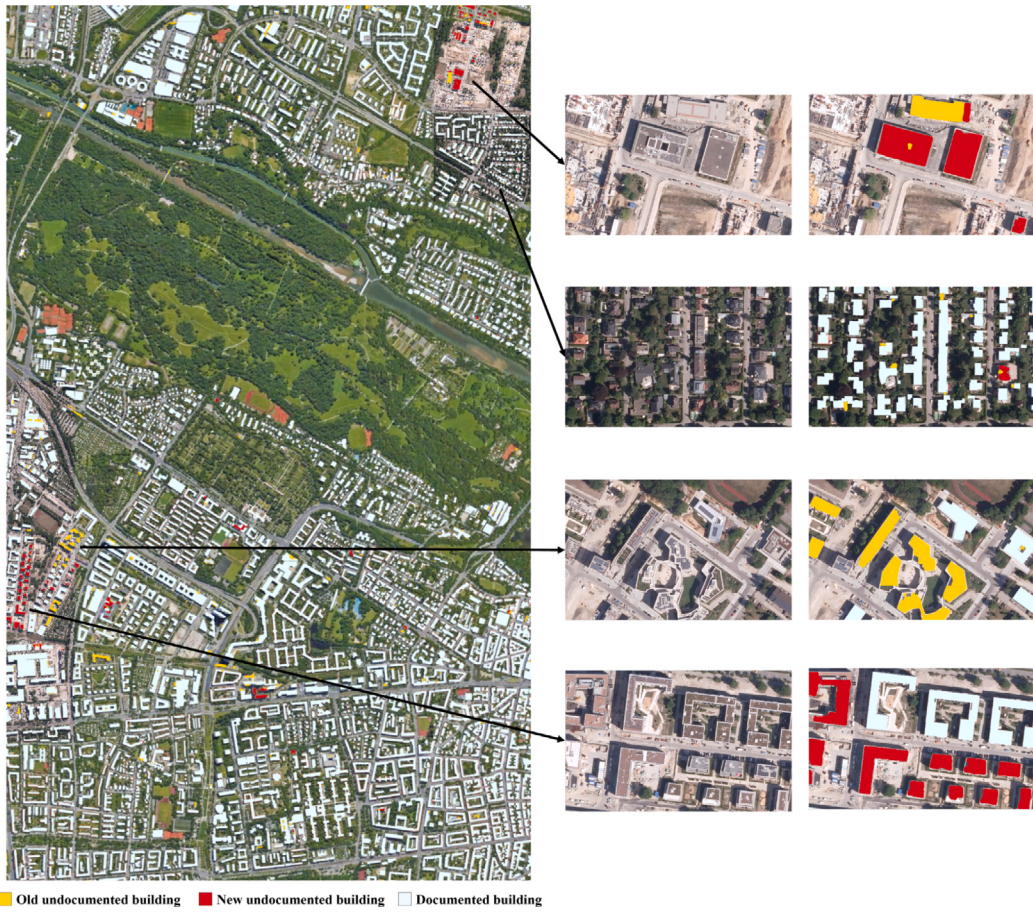


Fig. 4. Zoomed-in results of undocumented buildings for a sample urban area.

Table 5
Accuracies of different CNN models for building detection. (%)

Method	F1 score	IoU
FCN-8s (Long et al., 2015)	81.51 ± 0.62	68.84 ± 0.87
U-Net (Ronneberger et al., 2015)	81.99 ± 0.67	69.52 ± 0.94
DeepLab V3+ (Chen et al., 2018)	82.15 ± 0.53	69.69 ± 0.75
HA U-Net (Xu et al., 2021)	83.70 ± 0.36	72.17 ± 0.50
FC-DenseNet (Jégou et al., 2017)	85.14 ± 0.55	74.06 ± 0.77

evaluate building extraction results, we choose the city of Bad Toelz as test area, which covers 40 square kilometers. Its ground truth map has been manually checked to guarantee correctness. To verify the effectiveness of FC-DenseNet (Jégou et al., 2017) for building detection, we compare it with several commonly used network learning methods, i.e., FCN-8s (Long et al., 2015), U-Net (Ronneberger et al., 2015), DeepLab V3+ (Chen et al., 2018), and HA U-Net (Xu et al., 2021). Note that each experiment is carried out for five runs, which provides a fair comparison, and the corresponding F1 score and IoU are shown as mean and variance. Numerical results of building detection are shown in Table 5. We find that FC-DenseNet (Jégou et al., 2017) shows superior results in terms of F1 score and IoU when compared to all other networks applied. Specifically, FC-DenseNet (Jégou et al., 2017) obtains the F1 score of $85.14 \pm 0.5\%$ and the IoU of $74.06 \pm 0.77\%$. This demonstrates that FC-DenseNet (Jégou et al., 2017) is effective and robust in the task of building detection.

In our research, we generate undocumented building maps for 15 cities in the state of Bavaria. Fig. 4 illustrates a zoom-in visual example where documented buildings in the DFK, as well as undocumented buildings, have been identified by CNN. The buildings in yellow and red represent old and new undocumented buildings, respectively. When the tDSM shows no height deviation, these undocumented buildings

are classified as old undocumented buildings, indicating they were constructed before time point 1. When an obvious signal is identified in the tDSM, the undocumented buildings are classified as new undocumented buildings that were built between time point 1 and time point 2. To quantitatively evaluate the detected undocumented buildings, we check results in the city of Bad Toelz by manual photo interpretation. Specifically, 1271 undocumented buildings are correctly detected from our results (1545 undocumented buildings), and the precision is 82.27%. Note that the training data set of CNNs are collected in 14 cities excluding Bad Toelz. However, the implemented framework still offers satisfactory results in this city.

3.2. Morphology and landscape analysis of undocumented buildings

In order to investigate the spatial distribution of undocumented buildings, we define “high” and “low” density regions for each city. Based on the buildings predicted by the CNN, all cities are divided into five classes by the two selected clustering methods according to building density. Fig. 5 illustrates the building classification results of Muenchen that are obtained by K-means clustering and equal interval classification, respectively. For the results generated by K-means clustering, a region with a building density of $0.00 \sim 0.07$ is considered

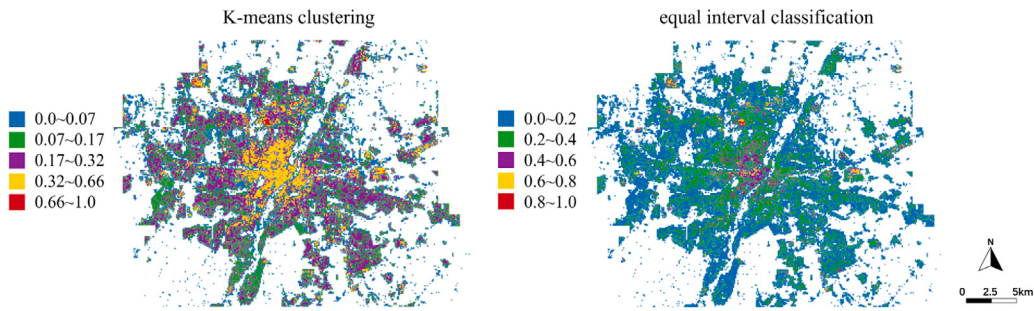


Fig. 5. Building density classification results of Muenchen obtained by K-means clustering and equal interval classification.



Fig. 6. (a), (c), and (e) are the share in the number, area, and volume of new undocumented buildings in different building density regions obtained by K-means clustering. (b), (d), and (f) are the number, area, and volume of new undocumented buildings in different building density regions obtained by equal interval classification.

very low, 0.07 ~ 0.17 is low, 0.17 ~ 0.32 is medium, 0.32 ~ 0.66 is high, and 0.66 ~ 1.0 is very high. While for the equal interval classification method, the ranges of very low, low, medium, high, and very high dense correspond to 0 ~ 0.2, 0.2 ~ 0.4, 0.4 ~ 0.6, 0.6 ~ 0.8, and 0.8 ~ 1.0, respectively.

The urban structure refers to the horizontal but also the vertical layout. Note that in our research, new undocumented buildings which were constructed between the year 2014 and the year 2017 are consid-

ered targets for further morphology and landscape analysis, facilitating the investigation of the urban development patterns.

3.2.1. State-scale investigation

The obtained result allows for localizing individual undocumented buildings and characterizing them in their physical appearance. To begin, however, we evaluate the effects on our metrics at an aggregated level with respect to the landscape structure. Fig. 6 consists of six pie charts, showing the number, area, and volume of new undocumented

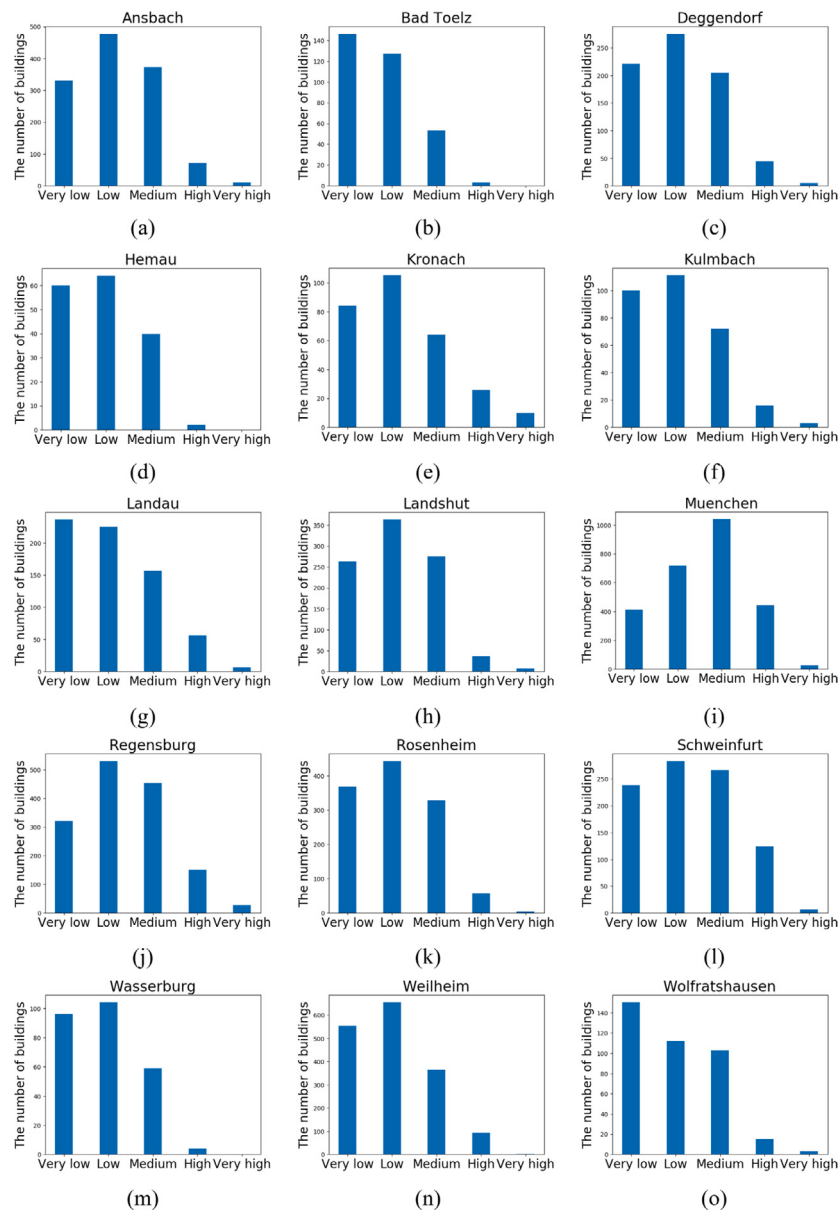


Fig. 7. The number of new undocumented buildings in different building density regions for (a) Ansbach, (b) Bad Toelz, (c) Deggendorf, (d) Hemau, (e) Kronach, (f) Kulmbach, (g) Landau, (h) Landshut, (i) Muenchen, (j) Regensburg, (k) Rosenheim, (l) Schweinfurt, (m) Wasserburg, (n) Weilheim, and (o) Wolfratshausen.

buildings for different building density regions for all 15 test cases. Although these pie charts are obtained from different clustering methods, it is interesting to note that they share a similar trend, i.e., more than half of the new undocumented buildings are identified in the very low and low building density regions (cf. Figs. 6(a) and (b)). This suggests that clustering method-dependent effects are able to be remedied. The same trend is also revealed by the building area and volume (i.e., very low and low dense regions have the largest share of undocumented buildings). This shows that the often-discussed fragmentation of the landscape and specifically urban sprawl in the peripheries of urban areas is obviously more advanced in Bavaria than it is depicted in official data sets such as the DFK. In addition, we have performed the analysis also on grid cells of 200 m × 200 m, and found that different grid sizes exert little influence on morphology and landscape analysis results.

3.2.2. City-scale investigation

In this section, we carry out the morphology and landscape analysis of undocumented buildings at the city scale. In this way, we are able to

explore whether the findings are in line with previous findings that the identified trend of a larger amount of undocumented buildings in lower dense areas is ubiquitous. Note that we utilize the K-means clustering method for the definition of high and low building density regions at the city-scale analysis, as K-means clustering and equal interval classification methods show a similar trend.

Fig. 7 illustrates the number of new undocumented buildings with respect to the different building density regions, covering 15 cities. Each subfigure shows a distribution of new undocumented buildings in a specific city. Looking at the spatial distribution of the number of buildings, we find that in most cities more undocumented buildings are identified in very low or low dense regions. This again indicates that urban sprawl in the state of Bavaria is probably greater than official geospatial data currently documented. An interesting finding is that Muenchen is the only city that has the largest number of undocumented buildings in the medium density class, with over 1000 buildings. Moreover, for different density regions, the numbers of undocumented buildings in Muenchen are larger than those in other cities. As an economic hub, Muenchen has experienced a high inward

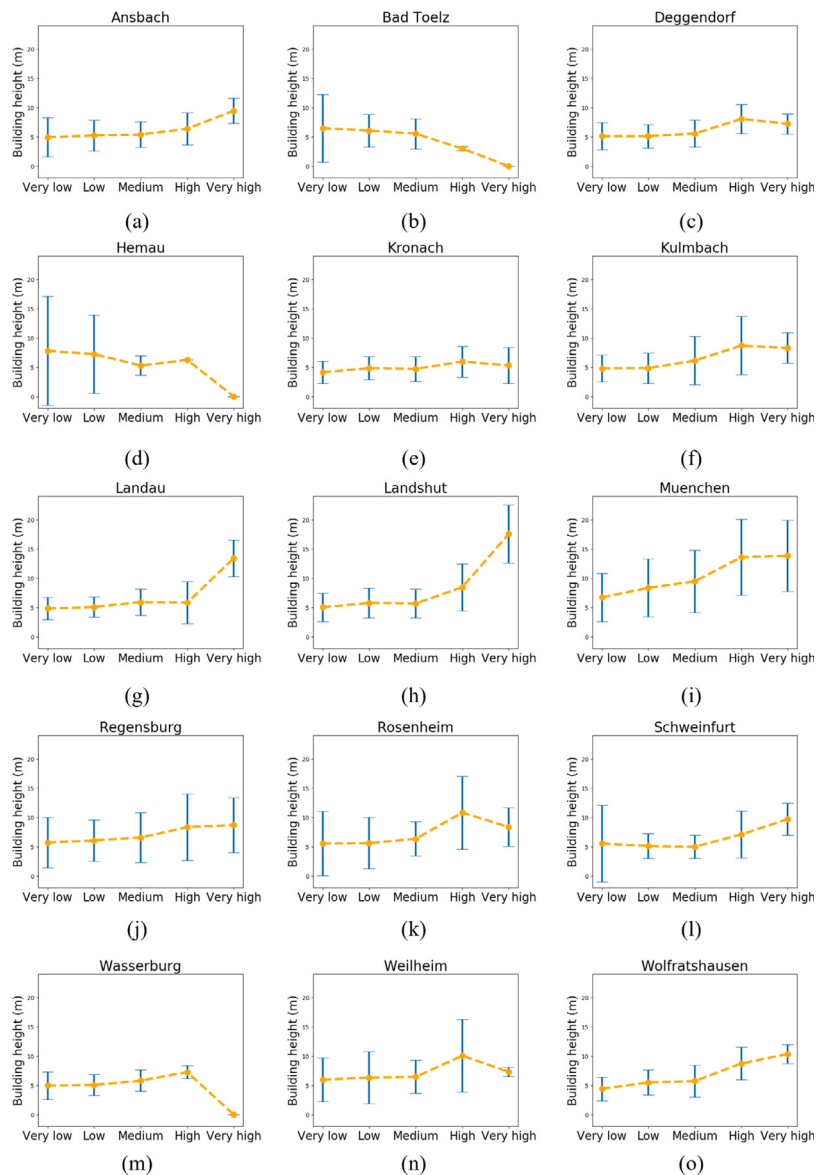


Fig. 8. The mean and standard deviation of building height of new undocumented buildings in different building density regions for (a) Ansbach, (b) Bad Toelz, (c) Deggendorf, (d) Hemau, (e) Kronach, (f) Kulmbach, (g) Landau, (h) Landshut, (i) Muenchen, (j) Regensburg, (k) Rosenheim, (l) Schweinfurt, (m) Wasserburg, (n) Weilheim, and (o) Wolfratshausen.

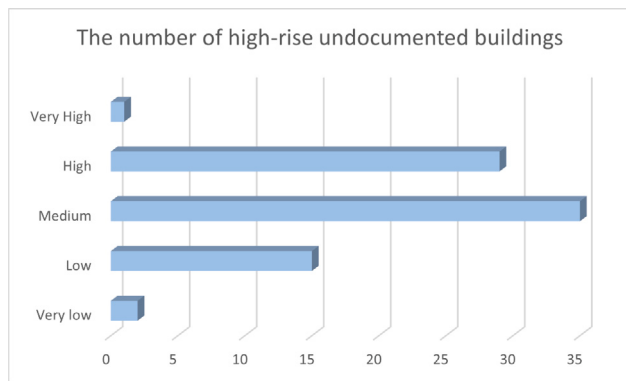


Fig. 9. The number of high undocumented buildings in different building density regions of Muenchen.

migration in the last years. The effect of high building construction dynamics, not yet documented in the DFK, are revealed by this analysis.

If two cities share similar 2D morphological parameters or landscape metrics, there might exist differences in 3D morphological parameters or landscape metrics. Fig. 8 illustrates the mean height and height deviation of undocumented buildings for different cities. For most cities, the mean height and height deviation of undocumented buildings in high density regions is larger than that in lower density regions. However, undocumented buildings of Bad Toelz and Hemau show smaller mean height and height deviation in high density regions than those in low density region. Height deviation depicts the height diversity of buildings. Large variations of building height in high density regions are owing to various factors such as building function types (e.g., commercial and residential areas) (Hu et al., 2016) and human activities (Li et al., 2020b).

In addition, the high-rise undocumented buildings in various cities are investigated (see Fig. 9). We generally find that higher buildings are specifically built in larger cities. In Muenchen there are 82 high and yet undocumented buildings identified, while in Regensburg – the

second largest city in our sample – it is only 18. In Muenchen we see the trend that these high buildings are predominantly built in the higher dense more central urban regions. This is related to building codes in urban planning. As medium and high density regions are near city centers where the land rent is high, newly built commercial buildings are usually high-rise office buildings, occupying fewer land (Wu et al., 2019).

4. Discussion

In this paper, we make use of the remote sensing data to investigate differences in cadastral data sets and up-to-date remote sensing data with respect to documented buildings at the scale of a federal state and a city. Specifically, we have identified undocumented buildings in official data sets and we compare their 2D and 3D morphological parameters and landscape metrics in different building density regions. By doing so, we are able to picture the spatial variability of undocumented buildings, allowing investigation of the structural building pattern.

Based on our study, we find that more than half of the undocumented buildings are located in lower dense regions. It reveals that landscape fragmentation and sprawl have progressed more than official geodata currently document. This is a crucial finding as adverse effects of fragmented living and sprawl have been documented in scientific studies. Examples are that more land consumption and higher budgets for infrastructure are needed. The benefits of the compact city to environmental and social development have been hinted by many studies (Zhao et al., 2020; Angel et al., 2020). Our analysis, however, reveals that in our test sites a compact design of redensification of cities is less extensive than the construction of buildings in lower dense areas.

In the following, the main outcomes of our study are critically discussed from various perspectives — data, methodology, and application:

(1) **data:** We make use of remote sensing data including the DSM and the TrueDOP, which permits the generation of 3D building models with high geometrical accuracies. The study shows that the CNN classification allows a detailed morphology and landscape analysis of undocumented buildings. Nevertheless, a major obstacle for similar large-scale applications is the acquisition of such datasets, which can be addressed by leveraging other remote sensing data sources. For instance, multi-view stereo satellite imagery, e.g., WorldView or Pleiades satellites can provide DSM and imagery with sub-meter resolution. The data provided by these satellites cover the whole globe in theory and are less expensive than airborne data. Still, their high revisit capability also helps to acquire low cloud cover observations for the regions with above-average cloud cover. However, for these very high resolutions data, costs are still an obstacle for large area, national, or even global applications. And beyond, multi-view stereo data are far from global availability.

(2) **methodology:** In this study, the detection of undocumented buildings relies heavily on building extraction results that are provided by the CNN. Therefore, related methodological challenges arising from the CNN need to be considered. According to the quantitative assessment of the accuracy of the building extraction results on the city of Bad Toelz, FC-DenseNet (Jégou et al., 2017) has achieved the highest accuracy when compared to the other four CNN models. FC-DenseNet (Jégou et al., 2017) achieves the F1 score of $85.14 \pm 0.55\%$ and the IoU of $74.06 \pm 0.77\%$, respectively. Of course, uncertainties remain despite the high accuracies, however, the CNN is superior to traditional methods in the task of large-scale building extraction, as the CNN is able to significantly alleviate false alarms (Li et al., 2020a). With respect to our work, any misclassification of buildings and non-building objects introduced by the CNN will result in questionable undocumented building detection results. Nevertheless, we find the undocumented building detection results are plausible in general, which are confirmed by the precision of undocumented buildings (82.27%).

For future research, we aim to explore more robust CNN models that are capable of improving building extraction results.

(3) **application:** The official building databases can be applied as a fundamental source to investigate the building structural patterns. Nevertheless, when building databases are not up-to-date, the derived morphological parameters and landscape metrics might be distorted. In other words, the morphology and landscape analysis of out-of-date building databases cannot provide valuable information to guarantee comprehensive urban planning and management. To overcome this issue, the focus of our study is to monitor undocumented buildings, which contributes to the construction of update-to-date building databases for valid building structural pattern analysis.

5. Conclusion and outlook

3D building models characterize the planar and vertical dimensions of urban structures, offering an insight into landscape structural development. However, official geodata sets in Germany are not always up-to-date so new approaches are needed to track the undocumented changes. The increasing availability of remote sensing data and CNN models provide great potential to spatiotemporally analyze undocumented buildings. In this study, we have established a set of 2D and 3D morphological parameters and landscape metrics in undocumented building analysis that can illustrate the current urban patterns. Our study reveals a disproportional distribution of undocumented buildings among different building density regions and a relatively high proportion of new undocumented buildings in lower dense regions. This suggests that landscape fragmentation and urban sprawl might be further developed than documented in official data sets in Germany. Moreover, we argue that up-to-date monitoring of the construction period, morphology, and landscape of undocumented buildings is demanded better-informed planning decisions. In the future, we will carry out research in different countries including both developed and developing countries. By analyzing their similarity and differences, we aim to better promote the international significance of our research.

CRediT authorship contribution statement

Qingyu Li: Conceptualization, Methodology, Software, Validation, Formal analysis, Investigation, Data curation, Writing – original draft, Writing – review & editing, Visualization. **Hannes Taubenböck:** Conceptualization, Methodology, Formal analysis, Writing – review & editing, Supervision. **Yilei Shi:** Methodology, Writing – review & editing, Supervision. **Stefan Auer:** Writing – review & editing, Project administration. **Robert Roschlau:** Writing – review & editing, Project administration. **Clemens Glock:** Data curation. **Anna Kruspe:** Project administration. **Xiao Xiang Zhu:** Resources, Writing – review & editing, Project administration, Funding acquisition.

Declaration of competing interest

The authors declare that they have no known competing financial interests or personal relationships that could have appeared to influence the work reported in this paper.

Acknowledgments

The work is jointly supported by the European Research Council (ERC) under the European Union's Horizon 2020 research and

innovation programme (grant agreement No. [ERC-2016-StG-714087], Acronym: So2Sat), by the Helmholtz Association, Germany through the Framework of Helmholtz AI (grant number: ZT-I-PF-5-01) - Local Unit “Munich Unit @Aeronautics, Space and Transport (MASTR)” and Helmholtz Excellent Professorship, Germany “Data Science in Earth Observation - Big Data Fusion for Urban Research”(grant number: W2-W3-100), by the German Federal Ministry of Education and Research (BMBF) in the framework of the international future AI lab “AI4EO – Artificial Intelligence for Earth Observation: Reasoning, Uncertainties, Ethics and Beyond” (grant number: 01DD20001) and by German Federal Ministry of Economics and Technology in the framework of the “national center of excellence ML4Earth” (grant number: 50EE2201C). This work is a part of the project “Investigation of building cases using AI” funded by Bavarian State Ministry of Finance and Regional Identity (StMFH), Germany and the Bavarian Agency for Digitization, High-Speed Internet and Surveying, Germany.

References

- Abdullahi, S., Pradhan, B., Mojaddadi, H., 2018. City compactness: Assessing the influence of the growth of residential land use. *J. Urban Technol.* 25 (1), 21–46.
- Angel, S., Franco, S.A., Liu, Y., Blei, A.M., 2020. The shape compactness of urban footprints. *Prog. Plan.* 139, 100429.
- Bonczak, B., Kontokosta, C.E., 2019. Large-scale parameterization of 3D building morphology in complex urban landscapes using aerial LiDAR and city administrative data. *Comput. Environ. Urban Syst.* 73, 126–142.
- Cao, S., Du, M., Zhao, W., Hu, Y., Mo, Y., Chen, S., Cai, Y., Peng, Z., Zhang, C., 2020. Multi-level monitoring of three-dimensional building changes for megacities: Trajectory, morphology, and landscape. *ISPRS J. Photogramm. Remote Sens.* 167, 54–70.
- Cao, Y., Huang, X., 2021. A deep learning method for building height estimation using high-resolution multi-view imagery over urban areas: A case study of 42 Chinese cities. *Remote Sens. Environ.* 264, 112590.
- Chen, Z., Xu, B., Devereux, B., 2014. Urban landscape pattern analysis based on 3D landscape models. *Appl. Geogr.* 55, 82–91.
- Chen, L.-C., Zhu, Y., Papandreou, G., Schroff, F., Adam, H., 2018. Encoder-decoder with atrous separable convolution for semantic image segmentation. In: Proceedings of the European Conference on Computer Vision (ECCV), pp. 801–818.
- Durieux, L., Lagabrielle, E., Nelson, A., 2008. A method for monitoring building construction in urban sprawl areas using object-based analysis of spot 5 images and existing GIS data. *ISPRS J. Photogramm. Remote Sens.* 63 (4), 399–408.
- Gefßler, S., Krey, T., Möst, K., Roschlaub, R., 2019. Mit Datenfusionierung Mehrwerte schaffen – Ein Expertensystem zur Baufallerkundung. *DVW-Mitteilungen* 2, 159–187.
- Griffiths, D., Boehm, J., 2019. Improving public data for building segmentation from convolutional neural networks (CNNs) for fused airborne lidar and image data using active contours. *ISPRS J. Photogramm. Remote Sens.* 154, 70–83.
- Hamidi, S., Ewing, R., 2014. A longitudinal study of changes in urban sprawl between 2000 and 2010 in the United States. *Landscl. Urban Plan.* 128, 72–82.
- Hartigan, J.A., Wong, M.A., 1979. Algorithm AS 136: A k-means clustering algorithm. *J. R. Stat. Soc. Ser. C* 28 (1), 100–108.
- Hu, T., Yang, J., Li, X., Gong, P., 2016. Mapping urban land use by using landsat images and open social data. *Remote Sens.* 8 (2), 151.
- Huang, X., Cao, Y., Li, J., 2020. An automatic change detection method for monitoring newly constructed building areas using time-series multi-view high-resolution optical satellite images. *Remote Sens. Environ.* 244, 111802.
- Huang, X., Li, J., Yang, J., Zhang, Z., Li, D., Liu, X., 2021. 30 M global impervious surface area dynamics and urban expansion pattern observed by Landsat satellites: From 1972 to 2019. *Sci. China Earth Sci.* 64 (11), 1922–1933.
- Huang, G., Liu, Z., Van Der Maaten, L., Weinberger, K.Q., 2017. Densely connected convolutional networks. In: Proceedings of the IEEE Conference on Computer Vision and Pattern Recognition, pp. 4700–4708.
- Huang, X., Song, Y., Yang, J., Wang, W., Ren, H., Dong, M., Feng, Y., Yin, H., Li, J., 2022. Toward accurate mapping of 30-m time-series global impervious surface area (GISA). *Int. J. Appl. Earth Obs. Geoinf.* 109, 102787.
- Jégou, S., Drozdzal, M., Vazquez, D., Romero, A., Bengio, Y., 2017. The one hundred layers tiramisu: Fully convolutional densenets for semantic segmentation. In: Proceedings of the IEEE Conference on Computer Vision and Pattern Recognition Workshops, pp. 11–19.
- Kontokosta, C.E., Tull, C., 2017. A data-driven predictive model of city-scale energy use in buildings. *Appl. Energy* 197, 303–317.
- Koohsari, M.J., Mavoa, S., Villanueva, K., Sugiyama, T., Badland, H., Kaczynski, A.T., Owen, N., Giles-Corti, B., 2015. Public open space, physical activity, urban design and public health: Concepts, methods and research agenda. *Health Place* 33, 75–82.
- Kubota, T., Miura, M., Tominaga, Y., Mochida, A., 2008. Wind tunnel tests on the relationship between building density and pedestrian-level wind velocity: Development of guidelines for realizing acceptable wind environment in residential neighborhoods. *Build. Environ.* 43 (10), 1699–1708.
- Leichtle, T., Geiß, C., Wurm, M., Lakes, T., Taubenböck, H., 2017. Unsupervised change detection in VHR remote sensing imagery—an object-based clustering approach in a dynamic urban environment. *Int. J. Appl. Earth Obs. Geoinf.* 54, 15–27.
- Li, Q., Shi, Y., Auer, S., Roschlaub, R., Möst, K., Schmitt, M., Glock, C., Zhu, X., 2020a. Detection of undocumented building constructions from official geodata using a convolutional neural network. *Remote Sens.* 12 (21), 3537.
- Li, X., Zhou, Y., Gong, P., Seto, K.C., Clinton, N., 2020b. Developing a method to estimate building height from sentinel-1 data. *Remote Sens. Environ.* 240, 111705.
- Liu, M., Hu, Y.-M., Li, C.-L., 2017. Landscape metrics for three-dimensional urban building pattern recognition. *Appl. Geogr.* 87, 66–72.
- Long, J., Shelhamer, E., Darrell, T., 2015. Fully convolutional networks for semantic segmentation. In: Proceedings of the IEEE Conference on Computer Vision and Pattern Recognition, pp. 3431–3440.
- Lu, C., Liu, Y., 2016. Effects of China's urban form on urban air quality. *Urban Stud.* 53 (12), 2607–2623.
- Lu, L., Weng, Q., Guo, H., Feng, S., Li, Q., 2019. Assessment of urban environmental change using multi-source remote sensing time series (2000–2016): A comparative analysis in selected megacities in eurasia. *Sci. Total Environ.* 684, 567–577.
- Ressl, C., Brockmann, H., Mandlburger, G., Pfeifer, N., 2016. Dense image matching vs. Airborne laser scanning—comparison of two methods for deriving terrain models. *Photogrammetrie-Fernerkundung-Geoinformation* 2016 (2), 57–73.
- Robinson, D., 2006. Urban morphology and indicators of radiation availability. *Sol. Energy* 80 (12), 1643–1648.
- Ronneberger, O., Fischer, P., Brox, T., 2015. U-net: Convolutional networks for biomedical image segmentation. In: International conference on medical image computing and computer-assisted intervention. Springer, pp. 234–241.
- Roschlaub, R., Möst, K., Krey, T., 2020. Automated classification of building roofs for the updating of 3D building models using heuristic methods. *PFG - J. Photogramm., Remote Sens. Geoinformation Sci.* 88.
- Said, K.A.M., Jambek, A.B., Sulaiman, N., 2016. A study of image processing using morphological opening and closing processes. *Int. J. Control Theory Appl.* 9 (31), 15–21.
- Taubenböck, H., Esch, T., Felbier, A., Wiesner, M., Roth, A., Dech, S., 2012. Monitoring urbanization in mega cities from space. *Remote Sens. Environ.* 117, 162–176.
- Taubenböck, H., Standfuß, I., Klotz, M., Wurm, M., 2016. The physical density of the city—Deconstruction of the delusive density measure with evidence from two European megacities. *ISPRS Int. J. Geo-Inf.* 5 (11), 206.
- Taubenböck, H., Standfuß, I., Wurm, M., Krehl, A., Siedentop, S., 2017. Measuring morphological polycentricity—a comparative analysis of urban mass concentrations using remote sensing data. *Comput. Environ. Urban Syst.* 64, 42–56.
- Tyner, J.A., 2014. Principles of Map Design. Guilford Publications.
- Wu, J., 2014. Urban ecology and sustainability: The state-of-the-science and future directions. *Landscl. Urban Plan.* 125, 209–221.
- Wu, J., Wang, S., Zhang, Y., Zhang, A., Xia, C., 2019. Urban landscape as a spatial representation of land rent: A quantitative analysis. *Comput. Environ. Urban Syst.* 74, 62–73.
- Xu, L., Liu, Y., Yang, P., Chen, H., Zhang, H., Wang, D., Zhang, X., 2021. Ha U-net: Improved model for building extraction from high resolution remote sensing imagery. *IEEE Access* 9, 101972–101984.
- Yoshida, H., Omae, M., 2005. An approach for analysis of urban morphology: methods to derive morphological properties of city blocks by using an urban landscape model and their interpretations. *Comput. Environ. Urban Syst.* 29 (2), 223–247.
- Zhao, F., Tang, L., Qiu, Q., Wu, G., 2020. The compactness of spatial structure in Chinese cities: Measurement, clustering patterns and influencing factors. *Ecosyst. Health Sustain.* 6 (1), 1743763.
- Zhou, D.-m., Xu, J.-c., Radke, J., Mu, L., 2004. A spatial cluster method supported by GIS for urban-suburban-rural classification. *Chinese Geograph. Sci.* 14 (4), 337–342.
- Zhu, X.X., Tuia, D., Mou, L., Xia, G.-S., Zhang, L., Xu, F., Fraundorfer, F., 2017. Deep learning in remote sensing: A comprehensive review and list of resources. *IEEE Geosci. Remote Sens. Magaz.* 5 (4), 8–36.